Hindawi
Advances in Meteorology
Volume 2022, Article ID 1999997, 13 pages
https://doi.org/10.1155/2022/1999997

Research Article

Variation in Surface Solar Radiation and the Influencing Factors in Xinjiang, Northwestern China

Lili Jin,[1,2] **Zhenjie Li**,[3,4,5] **Qing He**,[2] **and Alim Abbas**[2]

[1]*Department of Atmospheric Sciences, Yunnan University, Kunming 650500, China*
[2]*Institute of Desert Meteorology, China Meteorological Administration, Urumqi 830002, China*
[3]*State Key Laboratory of Desert and Oasis Ecology, Xinjiang Institute of Ecology and Geography, Chinese Academy of Sciences, Urumqi 830011, China*
[4]*University of Chinese Academy of Sciences, Beijing 100049, China*
[5]*Lincang Meteorological Bureau, Lincang 677099, China*

Correspondence should be addressed to Qing He; qinghe@idm.cn

Received 7 May 2022; Accepted 8 August 2022; Published 12 September 2022

Academic Editor: Pedro Jiménez-Guerrero

The variation of solar radiation has a profound effect on the surface energy balance and hydrological cycle. Although the relationship between solar radiation variation and its influencing factors has been extensively studied, they are seldom used in Xinjiang, the largest province in China. In this study, we investigated the spatial distribution and temporal variation in global radiation (*E*g), water vapor content (WVC), aerosol optical depth (AOD), total cloud cover (TCC), and low-level cloud cover (LCC) in Xinjiang, northwestern China, between 1961 and 2015. The annual average *E*g reported at all stations was 5126.3–6252.8 MJ·m^{-2} with a mean of 5672 MJ·m^{-2}. The highest annual mean E_g of 6252.8 MJ·m^{-2} occurred in Hami, eastern Xinjiang, whereas the lowest annual mean E_g of 5126.3 MJ·m^{-2} occurred in Urumqi, northern Xinjiang. The annual E_g variation was mainly affected by WVC, AOD, TCC, and LCC. Decreases in annual, spring, summer, autumn, and winter E_g trends were recorded in Xinjiang at rates of -33.88×10^{-2}, -1.92×10^{-2}, -1.89×10^{-2}, -3.47×10^{-2}, and -3.56×10^{-2} MJ·m^{-2}·decade^{-1}, respectively, with decreasing ratios of 9.43%, 5.85%, 0.14%, 8%, and 20.55%, respectively. Increasing trends in annual WVC, AOD, TCC, and LCC were noted in Xinjiang at rates of 7.12×10^{-5} mm·decade^{-1}, 2.74×10^{-6} decade^{-1}, 8.77×10^{-5} % decade^{-1}, and 5.73×10^{-5}% decade^{-1}, respectively. In addition, increasing trends in the annual E_g at Yining and Yanqi stations were observed. The E_g spatial distribution was complex in Xinjiang at the stations observed in this study, which were divided into six groups. E_g at group 1 showed an increasing trend associated with decreases in the WVC and TCC, whereas decreases in E_g were observed at groups 2–6, which could have been influenced by increases in AOD, TCC, and LCC.

1. Introduction

Global solar radiation is the main energy source at the Earth's surface and is the basis for all life worldwide. Moreover, it is an important factor in determining regional climates. Both the number of sunshine hours and the amount of global solar radiation are important physical quantities for assessing radiation conditions. Various studies analyzing global solar radiation have shown decreases in radiation in most parts of the world from the 1950s to the 1990s [1–5]. In addition, many studies have reported variation in the solar radiation in China. Liang et al. [6] found that global solar radiation and direct radiation exhibited decreasing trends from 1961 to 2000, and Yang et al. [7] reported that the global solar radiation decreased by ~8% between 1961 and 2002. Streets et al. [8] found a decrease of 2.7–5.7 W·m^{-2}·decade^{-1} in the global solar radiation during 1960–2000, whereas Che et al. [9] reported a decrease of 4.5 W·m^{-2}·decade^{-1} during the same period based on data obtained from 64 sites. Moreover, Qian et al. [10] reported a decrease in the global solar radiation of 3.1 W·m^{-2}·decade^{-1} from 1955 to 2000 based on data obtained from 85 sites; Shi et al. [11] found a more pronounced decrease of 4.6% decade^{-1} between 1961 and 1989; and Zou et al. [12] reported

that a decrease in global solar radiation occurred at a rate of -2.11×10^{-3} MJ·m^{-2}·decade^{-1} in Hunan province during 1980–2013. The radiation tended to exhibit a more gradual decreasing trend in the northern, northeastern, and southwestern areas than in other areas of China [13]. In addition, Chen et al. [14] reported that the global solar radiation decreased -0.38 MJ·m^{-2}·day^{-1} 10 years^{-1} in Xinjiang from 1961 to 2000.

Many factors, such as dimensions of cloud coverage, altitude, and the presence of aerosols, affect the ability of global solar radiation to reach the Earth's surface. Li et al. [15] estimated the global solar radiation at 116 stations and reported that the main factors affecting the global solar radiation at the Qinghai-Tibet Plateau were local cloud coverage and altitude. He et al. [16] reported that global solar radiation in the hinterland of the Taklimakan Desert was significantly weakened by cloud coverage, cloud shape, and very fine sand particles. It has been suggested that this decreasing trend in global radiation (E_g) was caused by an increase in suspended particles. The global solar radiation reaching the Earth's surface has significantly decreased during the past 50 years by 0.51 ± 0.05 W·m^{-2}·year^{-1}, which is equivalent to a decrease of 2.7% per decade. This is attributed mainly to increases in aerosols and other pollutants, which changed the optical properties of the atmosphere [4]. Wild [17] suggested that the major modulator in China during the first half of the global solar radiation trend during 1971–1989 was aerosols, whereas that during the second half during 1990–2002 was cloud cover reduction. The question of which modulator had the highest contribution to changes in global solar radiation remains unclear based on previous research because the relative importance of aerosols, clouds, and aerosol-cloud interactions can differ, depending on the region and pollution level [18].

Observational E_g data are scarce despite the existing radiation estimation models and satellite remote sensing data, which provide useful methods for studying regional radiation as well as E_g. The estimates of global solar radiation are based mainly on sunshine hours, water vapor, and atmospheric optical properties [19–22]. Inversion of global solar radiation based on satellite remote sensing can provide detailed spatial distribution information of the surface energy in large regions and facilitates assimilation of observational data from sparse ground sites into large areas [23]. The use of satellite data to estimate global solar radiation began in the 1960s and includes statistical and physical inversion methods [24–26]. Many researchers have since used the observational data from ground stations and satellite data to study terrestrial global solar radiation. Such research includes the spatial and temporal distribution characteristics of global solar radiation and their influencing factors [27–29]. The scope of previous studies has expanded from a particular region to national and global levels [1, 5, 30–32]. In addition, previous research includes the distribution characteristics of solar radiation in the Xinjiang region. Zhou et al. [33] studied the global solar radiation in Xinjiang based on surface observations and data of the National Aeronautics and Space Administration/Global Energy and Water Exchanges (NASA/GEWEX) Surface Radiation Budget (SRB) retrieved from satellites. In their study, the solar radiation retrieved by the NASA/GEWEX SRB program was shown to be about 10%–30% greater than that estimated from observational data.

The vast territory of Xinjiang includes different terrain and climatic conditions that strongly affect the radiation; the influences of latitude and solar altitude are also important. Previous research on E_g in Xinjiang has paid little attention to the particular conditions at different sites. The factors that affect the ability of global solar radiation to reach the Earth's surface in Xinjiang have been less studied; thus, the relationship between global solar radiation and its potential causal factors remains unclear. Therefore, it is important to determine the factors affecting global solar radiation in Xinjiang.

The main objective of this study was to investigate the long-term trend of global solar radiation in Xinjiang province during 1961–2015. The global solar radiation and its main influencing factors during this period for each station in Xinjiang province were analyzed based on the spatial differences in the variation of global solar radiation. Moreover, the global solar radiation and its correlations with the total cloud cover (TCC), low-level cloud cover (LCC), water vapor content (WVC), and aerosol optical depth (AOD) were calculated to determine the influences of variations in the global solar radiation.

2. Data and Methodology

The study region is Xinjiang province (73.66 E–96.38 E, 34.42 N–49.17 N) in northwestern China (Figure 1). Its area of 1.66×10^6 km^2 accounts for 16.6% of the country's total area, which makes Xinjiang the largest province in China. This region has complex topography including plateaus; large mountains; sediment basins including the Tarim, Junggar, and Turpan basins; the Gobi desert; and oases. The complex landform of "three mountains and two basins," including the Altai, Tianshan, and Kunlun mountains and Junggar and Tarim basins, has formed a complex and diverse climate in Xinjiang [34]. The typical arid climate of the region is associated with these landscape characteristics. In particular, the region has considerable water and soil photothermal resources as well as long days. The accumulated temperature, temperature differences between day and night, frost-free periods, and annual solar radiation are all high and second only to those in Tibet. Therefore, Xinjiang is rich in solar thermal resources. In addition, the region has abundant sunshine and heat as well as low precipitation with uneven spatial and temporal distributions [35, 36].

The hourly and daily surface meteorological data recorded at 11 stations in Xinjiang province including Altai, Tacheng, Yining, Urumqi, Turpan, Hami, Yanqi, Ruoqiang, Aksu, Kashgar, and Hetian stations were obtained from the Xinjiang Meteorological Data Center.

The data of continuously observed daily E_g; annual mean E_g; WVC; temperature (T); TCC; LCC; visibility at 00 : 00, 06 : 00, 12 : 00, and 18 : 00 LTC; and number of days with dust present recorded by the 11 stations in Xinjiang were retrieved for the period 1961–2015. The daily E_g exposure at

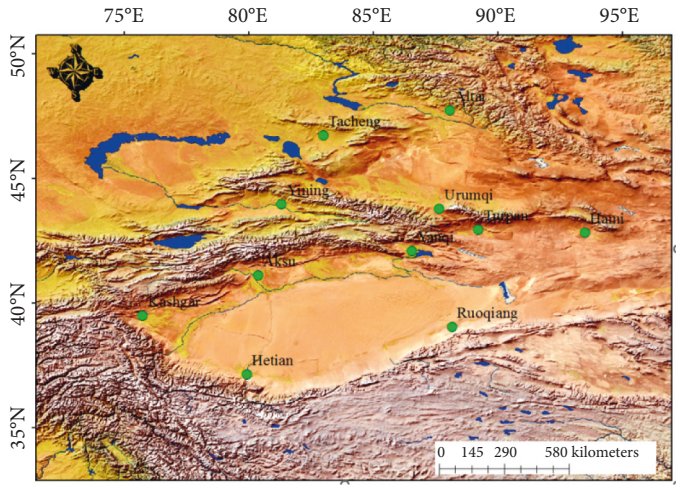

Figure 1: Study area and stations in Xinjiang province.

all stations is given in units of megajoules per meter. The monthly average was calculated from the daily data, whereas the seasonal average was calculated from the monthly average.

The annual mean E_g values were 5504.8, 5609.2, 5423.2, 5126.3, 5654.9, 6103.3, 5489.9, 5713.9, 5904.9, 5608.9, and 6252.8 MJ·m^{-2} at the Altai, Tacheng, Yining, Urumqi, Yanqi, Ruoqiang, Aksu, Kashgar, Hetian, Turpan, and Hami stations, respectively. The annual mean E_g in Xinjiang ranged from 5126 to 6253 MJ·m^{-2}, with higher (lower) levels of radiation recorded in the south and east (north and west). The highest value was observed at the Hami station in eastern Xinjiang, whereas the lowest value was observed at the Urumqi station.

Prior to 1993, the radiation observation instruments used at all stations in China were manganin-constantan thermocouple arrays, which included a Soviet style radiometer with an induction surface coated with ordinary black paint. The data of these instruments and had relative error of 10%. Since that time, all stations in China have used a different type of thermoelectric instrument using copper-plated continuous coil and an induction surface with reflective black paint as a fully automatic telemetry radiometer giving data with relative error of 0.5% [14].

Operation-related problems, zero drift of the sensor, measurement error, and varying degrees of missing data occur in the long-term and continuous radiometer observations in Xinjiang. Thus, to guarantee consistency, quality control processes were implemented including zero drift correction, extreme value checks, consistency checks, and similarity checks. Moreover, the uniformity of radiation data has been examined, and the outliers, such as missing values higher than the astronomical radiation and negative values, were eliminated [37, 38].

In this study, the TCC, which is the proportion of the sky covered by clouds, and LCC were determined on a scale of 0–10 oktas. The logical extreme check, station-by-station spatial correlation check, time consistency check, spatial consistency check, and objective test quality control methods were applied to analyze the observation E_g data.

In the analysis, the AOD was calculated by the following equations [39, 40]:

$$\delta(\lambda) = \left(\frac{3.912}{V} - 0.0116\right)\left(\frac{0.55}{\lambda}\right)^{2-v^*} \times \left[H_1\left(e^{-(z/H_1)} - e^{-(5.5/H_1)}\right) + 12.5e^{-(5.5/H_1)} + H_2 e^{-(5.5/H_1)}\right] f, \quad (1)$$

$$f = e^{(0.42+0.0046P_w+0.015V_z)} \exp\left(-0.0047V_Z^2/P_w\right), \quad (2)$$

$$V_Z = \frac{3.912}{\left[0.0116 - 0.00099Z + ((3.912/V) - 0.0116)e^{-(z/0.886+0.0222V)}\right]}, \quad (3)$$

$$P_w = 0.6107e^{(17.33T/(239+T))} \times \mathrm{RH}, \quad (4)$$

where $\delta(\lambda)$ is the AOD value, λ (= 0.55 μm) is the wavelength, V is the visibility at sea level, $V^* = -2$, $H_1 = 0.886 + 0.0222$ V(km), $H_2 = 3.77$ km, f is the correction coefficient, P_w is the ground water vapor pressure (hPa), and z is altitude (km). Specifically, where T is the surface temperature (°C) and RH is the relative humidity (%) [41].

3. Results

3.1. Trends of E_g, LCC, TCC, AOD, and WVC and Their Relationships

3.1.1. Variation in E_g. Figures 2 and 3 show the annual and seasonal trends of E_g, TCC, LCC, WVC, and AOD as well as their smoothed line based on the robust locally weighted Lowess regression algorithm. The annual mean E_g values were 16.83 $MJ{\cdot}m^{-2}{\cdot}day^{-1}$ in the 1960s, 16.37 $MJ{\cdot}m^{-2}{\cdot}day^{-1}$ in the 1970s, 15.68 $MJ{\cdot}m^{-2}{\cdot}day^{-1}$ in the 1980s, 15.54 $MJ{\cdot}m^{-2}{\cdot}day^{-1}$ in the 1990s, 15.28 $MJ{\cdot}m^{-2}{\cdot}day^{-1}$ in the 2000s, and 15.35 $MJ{\cdot}m^{-2}{\cdot}day^{-1}$ in the 2010s. A decreasing trend in the annual E_g at a rate of -33.88×10^{-2} $MJ{\cdot}m^{-2}$ $decade^{-1}$ was observed in Xinjiang province during 1961–2015, showing a decrease of 9.43% (Table 1). The annual mean global solar radiation decreased in northwestern China during 1961–2005 [42]. The annual E_g strongly decreased during 1961–1992 at a rate of -0.60 $MJ{\cdot}m^{-2}decade^{-1}$ in Xinjiang; afterward, the annual E_g weakly decreased during 1993–2015 at a rate of -0.22 $MJ{\cdot}m^{-2}decade^{-1}$. The seasonal mean E_g values were 1.65, 2.00, 1.18, and 0.78 $MJ{\cdot}m^{-2}{\cdot}day^{-1}$ in the 1960s and 1.57, 1.91, 1.04, and 0.62 $MJ{\cdot}m^{-2}{\cdot}day^{-1}$ in the 2010s in spring, summer, autumn, and winter, respectively. As shown in Table 2, the annual E_g values decreased in spring, summer, autumn, and winter at rates of -1.92×10^{-2}, -1.89×10^{-2}, -3.47×10^{-2}, and -3.56×10^{-2} $MJ{\cdot}m^{-2}decade^{-1}$, respectively, representing decreases of 5.85%, 0.14%, 8%, and 20.55%, respectively.

3.1.2. Relationship between E_g and LCC. The annual mean LCC values were 5.7%, 4.7%, 5.4%, 8.9%, 12.6%, and 14.9% in the 1960s, 1970s, 1980s, 1990s, 2000s, and 2010s, respectively. An increasing trend in the annual LCC at a rate of 5.73×10^{-5}% $decade^{-1}$ was observed during 1961–2015 in Xinjiang province (Table 1). Further analysis revealed that the annual LCC decreased during 1961–1990 at a rate of -3.73×10^{-4}% $decade^{-1}$; afterward, the LCC increased during 1991–2015 at a rate of 8.84×10^{-3}% $decade^{-1}$. The seasonal mean LCC values were 1.31×10^{-2}, 3.33×10^{-2}, 1.06×10^{-2}, and 0.68×10^{-2}% day^{-1} the 1960s and 3.83×10^{-2}, 5.96×10^{-2}, 3.62×10^{-2}, and 3.12×10^{-2}% day^{-1} in the 2010s for spring, summer, autumn, and winter, respectively. The annual LCC increased in spring, summer, autumn, and winter at rates of 5.95×10^{-4}, 6.22×10^{-4}, 5.64×10^{-4}, and 5.12×10^{-4}% $decade^{-1}$ (Table 1). Significant negative correlations were noted between E_g and TCC, with correlation coefficients of −0.226 for the annual period and −0.311, −0.386, −0.259, and −0.372 for spring, summer, autumn, and winter, respectively. This indicates that dimming in Xinjiang province was likely caused by increases in the TCC during 1961–2015, particularly in spring, summer, and winter.

3.1.3. Relationship between E_g and TCC. The annual mean TCC values were 45.9%, 46.1%, 46.4%, 45.3%, 46.0%, and 49.2% in the 1960s, 1970s, 1980s, 1990s, 2000s, and 2010s, respectively. Moreover, increasing trends for the annual TCC were observed in Xinjiang province during 1961–2015 at a rate of 8.77×10^{-5}% $decade^{-1}$ (Table 1). The seasonal mean TCC values were 1.57×10^{-1}, 1.35×10^{-1}, 1.04×10^{-1}, and 1.24×10^{-1}% day^{-1} in the 1960s and 1.52×10^{-1}, 1.48×10^{-1}, 1.16×10^{-1}, and 1.38×10^{-1}% day^{-1} in the 2010s for spring, summer, autumn, and winter, respectively. The annual TCC increased in summer, autumn, and winter at rates of 1.12×10^{-4}, 1.64×10^{-4}, and 1.67×10^{-4}% $decade^{-1}$, respectively, but decreased in spring at a rate of -2.11×10^{-4}% $decade^{-1}$ (Table 1).

Negative (positive) trends of E_g (LCC) were observed for the annual period and all seasons (Figure 2). As shown in Table 1, significant negative correlations were noted between E_g and LCC, with correlation coefficients of −0.612 for the annual period and −0.333, −0.194, −0.754, and −0.646 for spring, summer, autumn, and winter, respectively. This indicates that dimming in Xinjiang province was likely caused by increase in the LCC during 1991–2015, particularly in autumn and winter.

3.1.4. Relationship between E_g and AOD. The annual mean AOD values were 0.87, 0.92, 0.77, 0.68, 0.87, and 1.01 in the 1960s, 1970s, 1980s, 1990s, 2000s, and 2010s, respectively. The annual mean AOD showed an increasing volatility trend during 1961–2015 at a rate of $2.74\times10^{-6}{\cdot}decade^{-1}$ (Table 1). The seasonal mean TCC values were 1.57×10^{-1}, 1.35×10^{-1}, 1.04×10^{-1}, and 1.24×10^{-1}%$\cdot day^{-1}$ in the 1960s and 1.52×10^{-1}, 1.48×10^{-1}, 1.16×10^{-1}, and 1.38×10^{-1}% day^{-1} in the 2010s for spring, summer, autumn, and winter, respectively. The annual TCC increased in summer, autumn, and winter at rates of 1.12×10^{-4}, 1.64×10^{-4}, and 1.67×10^{-4}% $decade^{-1}$, respectively, but decreased in spring at a rate of -2.11×10^{-4}%$\cdot decade^{-1}$ (Table 1).

3.2. Trends of E_g, TCC, LCC, AOD, and WVC at Each Station.

Figure 4 shows the distributions of the E_g, TCC, LCC, AOD, and WVC trends at each station. The E_g at nine stations showed decreasing trends, whereas the Yining and Yanqi stations showed increasing trends distributed mainly in the central area of Xinjiang (Figure 4(a)). Of the eleven stations, seven showed decreasing trends in the WVC (Figure 4(b)), and four showed decreasing trends in the AOD (Figure 4(c)). The Yining and Hami stations showed decreasing trends in the LCC (Figure 4(d)), whereas the Yining, Yanqi, and Urumqi stations showed decreasing trends in the TCC (Figure 4(e)).

Further analysis revealed that the Aksu, Kashgar, Hetian, and Ruoqiang stations and the Altai, Tacheng, and Urumqi stations located south and north of the Tianshan Mountains, respectively, showed decreases in the E_g and increases in the TCC and LCC (Figures 4(a), 4(d), and 4(e)). The Yining and Yanqi stations showed an increasing trend in E_g and decreasing trends in the WVC and LCC.

Table 2 shows the multiyear mean of the E_g for all stations, which ranged from 14.04 to 17.08 $MJ{\cdot}m^{-2}{\cdot}decade^{-1}$ at the Urumqi and Hami stations, respectively. The multiyear mean of the WVC ranged from 0.025 to 0.036 $mm{\cdot}decade^{-1}$at the Altai and Yining stations,

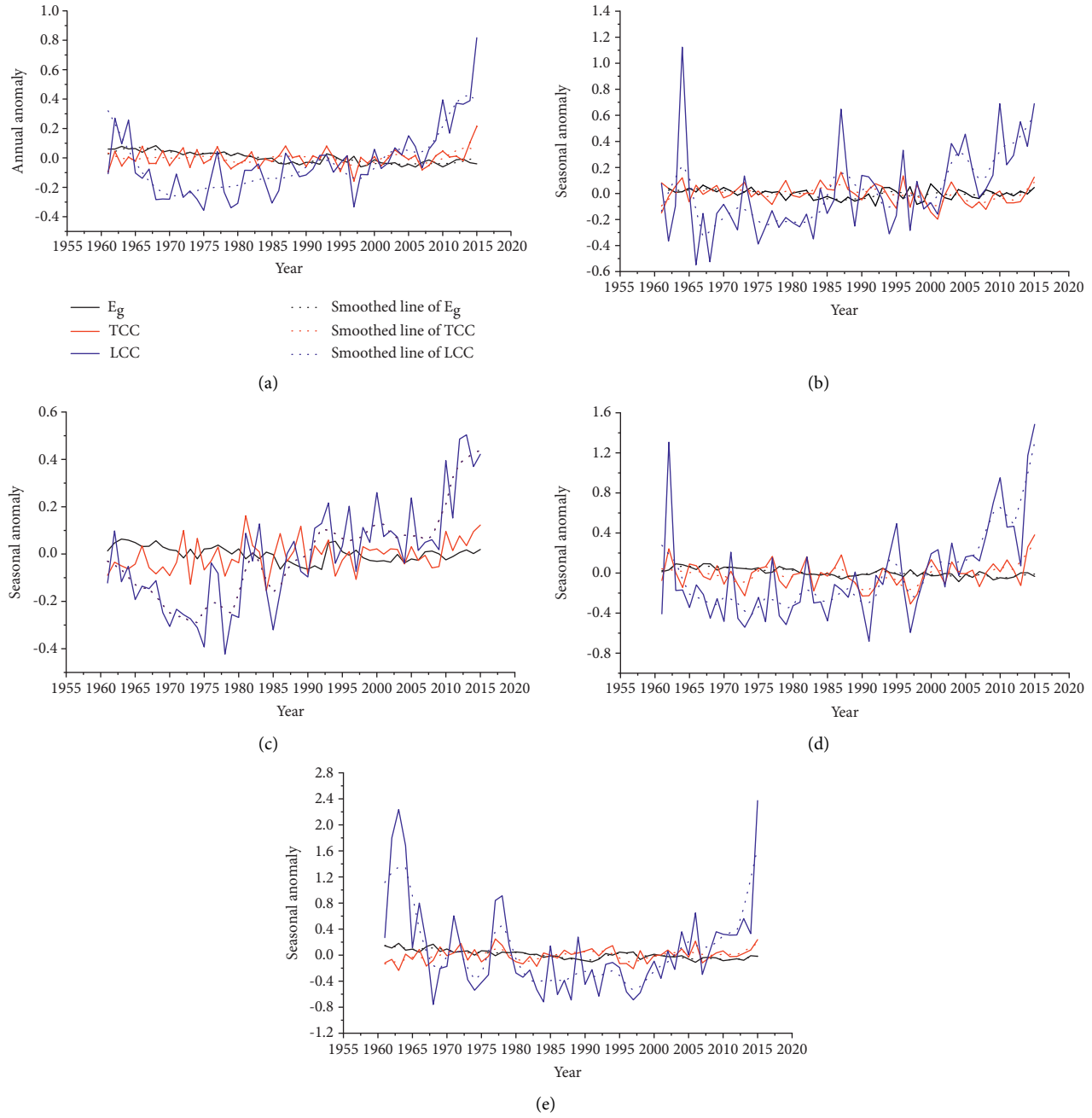

FIGURE 2: Interannual variations in the anomalies of E_g (black solid lines), TCC (red solid lines), and LCC (blue solid lines) smoothed (dashed lines) by using the Lowess robust locally weighted regression algorithm. (a) Annual. (b) Spring. (c) Summer. (d) Autumn. (e) Winter.

respectively, and that of the AOD ranged from 0.0011 to 0.0051·decade^{-1} at the Hami and Urumqi stations, respectively. The multiyear mean of the TCC ranged from 0.114% to 0.146% decade^{-1} at the Turpan and Altai stations, respectively, and that of the LCC ranged from 0.004% to 0.064% decade^{-1} at the Ruoqiang and Tacheng stations, respectively.

The decreasing trends of the E_g ranged from -6.42×10^{-1} to -1.28×10^{-1} MJ·m^{-2}·decade^{-1} at the Tacheng and Hetian stations, respectively, whereas its increasing trends were between 1.14×10^{-1} MJ·m^{-2} decade^{-1} at the Yining station and 1.87×10^{-1} MJ·m^{-2} decade^{-1} at the Yanqi station. The highest decreasing trends in the WVC, AOD, TCC, and LCC were -33.70×10^{-4} mm·decade^{-1}, -4.11×10^{-4}·decade^{-1}, -1.48×10^{-3}%·decade^{-1}, and -3.21×10^{-3}%·decade^{-1} at the Aksu, Turpan, Turpan, and Hami stations, respectively. The highest increasing trends were 9.32×10^{-4} mm·decade^{-1}, 33.97×10^{-4}·decade^{-1}, 17.04×10^{-3}%·decade^{-1}, and 15.51×10^{-3}%·decade^{-1}at the Ruoqiang, Urumqi, Aksu, and Yanqi stations, respectively (Table 2).

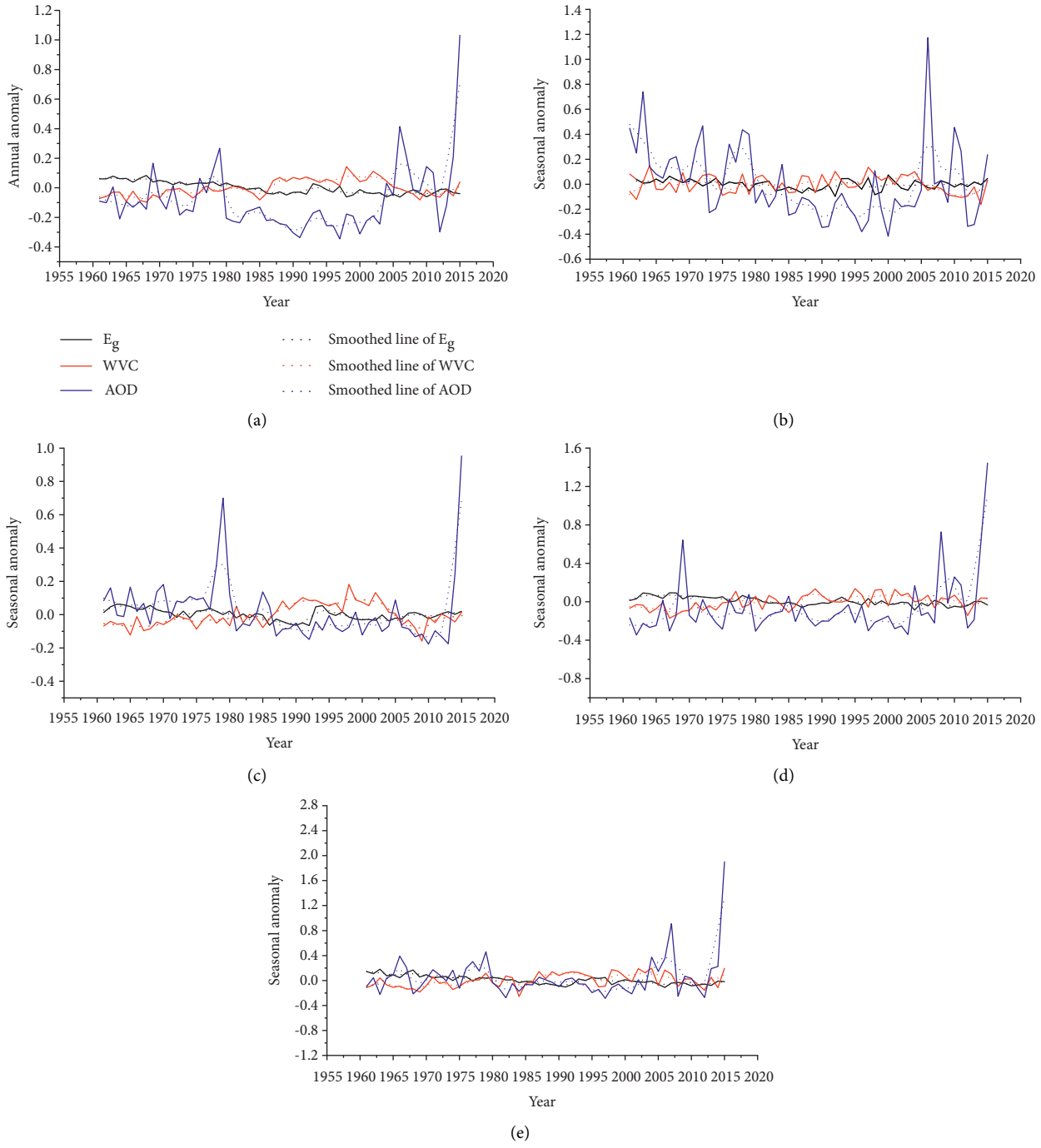

Figure 3: Interannual variations in anomalies of E_g (black solid lines), WVC (red solid lines), and AOD (blue solid lines) smoothed (dashed lines) by using the Lowess algorithm. (a) Annual. (b) Spring. (c) Summer. (d) Autumn. (e) Winter.

Table 1: Annual and seasonal trends in E_g, WVC, AOD, TCC, and LCC per decade and their correlation coefficients.

	ANN	MAM	JJA	SON	DJF
Trend					
E_g (MJ m^{-2})	$\mathbf{-33.88\times10^{-2}}$	$\mathbf{-1.92\times10^{-2}}$	$\mathbf{-1.89\times10^{-2}}$	$\mathbf{-3.47\times10^{-2}}$	$\mathbf{-3.56\times10^{-2}}$
WVC (mm)	$\mathbf{7.12\times10^{-5}}$	3.01×10^{-5}	6.85×10^{-5}	$\mathbf{5.48\times10^{-5}}$	$\mathbf{2.74\times10^{-5}}$
AOD	2.74×10^{-6}	-2.74×10^{-5}	-1.92×10^{-5}	1.37×10^{-5}	$\mathbf{4.66\times10^{-5}}$
LCC (%)	5.73×10^{-5}	$\mathbf{5.95\times10^{-4}}$	$\mathbf{6.22\times10^{-4}}$	$\mathbf{5.64\times10^{-4}}$	$\mathbf{5.12\times10^{-4}}$
TCC (%)	8.77×10^{-5}	$\mathbf{-2.11\times10^{-4}}$	1.12×10^{-4}	1.64×10^{-4}	1.67×10^{-4}

Table 1: Continued.

	ANN	MAM	JJA	SON	DJF
Correlation coefficients					
WVC	**−0.662**	−0.158	**−0.478**	**−0.660**	**−0.593**
AOD	−0.048	0.093	0.252	**−0.345**	**−0.462**
LCC	**−0.612**	**−0.333**	−0.194	**−0.754**	**−0.646**
TCC	−0.226	**−0.311**	**−0.386**	−0.259	**−0.372**

Note. ANN: annual period; MAM: March through April (spring); JJA: June through August (summer); SON: September through November (autumn); and DJF: December through January (winter). Bold values indicate trends significant at the 95% level.

Table 2: Annual mean daily values of E_g, WVC, AOD, TCC, and LCC and their long-term trends (A) recorded at each station from 1961 to 2015.

Station	Alt	E_g	WVC	AOD	TCC	LCC	A (E_g)	A (WVC)	(AOD)	(TCC)	(LCC)
Altai	735.1	15.08	0.025	0.0018	0.146	0.029	-2.13×10^{-1}	6.85×10^{-4}	-0.82×10^{-4}	0.33×10^{-3}	$\mathbf{2.11\times10^{-3}}$
Tacheng	555.0	15.37	0.029	0.0027	0.130	0.064	-6.42×10^{-1}	-11.51×10^{-4}	4.66×10^{-4}	2.22×10^{-3}	$\mathbf{13.78\times10^{-3}}$
Yining	663.0	14.86	0.036	0.0023	0.134	0.052	1.14×10^{-1}	-11.34×10^{-4}	5.75×10^{-4}	-1.04×10^{-3}	-3.01×10^{-3}
Urumqi	935.0	14.04	0.027	0.0051	0.126	0.056	-3.58×10^{-1}	-6.30×10^{-4}	33.97×10^{-4}	3.97×10^{-3}	7.90×10^{-3}
Yanqi	1055.8	15.49	0.032	0.0021	0.117	0.048	1.87×10^{-1}	-11.51×10^{-4}	16.44×10^{-4}	-0.22×10^{-3}	$\mathbf{15.51\times10^{-3}}$
Ruoqiang	888.3	16.72	0.026	0.0025	0.119	0.004	-1.68×10^{-1}	$\mathbf{9.32\times10^{-4}}$	1.64×10^{-4}	0.14×10^{-3}	$\mathbf{0.66\times10^{-3}}$
Aksu	1103.8	15.04	0.034	0.0014	0.129	0.039	-4.31×10^{-1}	$\mathbf{-33.70\times10^{-4}}$	0	17.04×10^{-3}	$\mathbf{15.42\times10^{-3}}$
Kashgar	1289.0	15.65	0.031	0.0016	0.138	0.030	-2.30×10^{-1}	2.19×10^{-4}	$\mathbf{-1.10\times10^{-4}}$	$\mathbf{4.47\times10^{-3}}$	$\mathbf{8.11\times10^{-3}}$
Hetian	1374.6	16.16	0.029	0.0024	0.125	0.006	-1.28×10^{-1}	0	-1.10×10^{-4}	0.16×10^{-3}	1.15×10^{-3}
Turpan	34.5	15.37	0.032	0.0037	0.114	0.017	$\mathbf{-4.67\times10^{-1}}$	-3.01×10^{-4}	$\mathbf{-4.11\times10^{-4}}$	-1.48×10^{-3}	$\mathbf{1.51\times10^{-3}}$
Hami	737.9	17.08	0.026	0.0011	0.120	0.016	-4.08×10^{-1}	6.85×10^{-4}	0	2.88×10^{-3}	$\mathbf{-3.21\times10^{-3}}$

Note. ALT: altitude at mean sea level. Bold values indicate trends significant at the 95% level. Units: E_g: MJ m^{-2}·decade^{-1}; WVC: mm; LCC: %; and TCC: %.

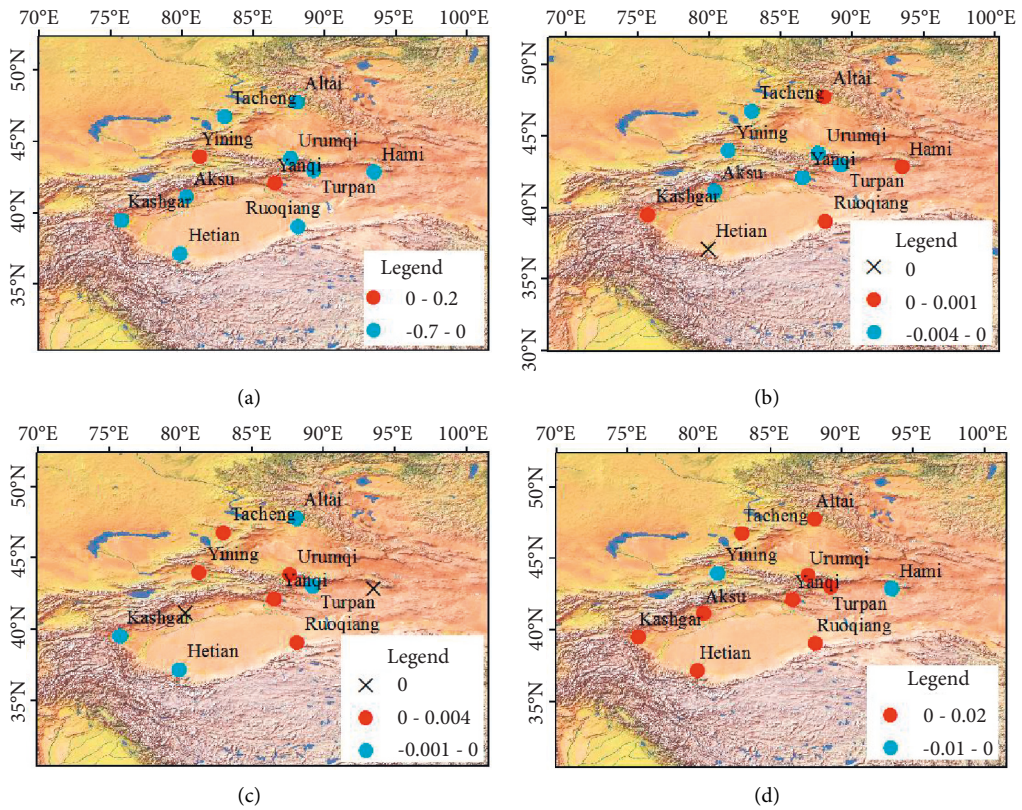

Figure 4: Continued.

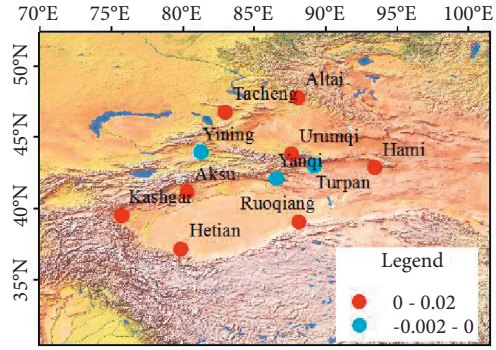

(e)

FIGURE 4: Trend of variability in Xinjiang recorded during 1961–2015. (a) E_g (MJ m^{-2} decade^{-1}); (b) WVC (mm decade^{-1}); (c) AOD (decade^{-1}); (d) LCC (% decade^{-1}); and (e) TCC (% decade^{-1}).

Six groups were classified in this study according to the long-term trends of E_g, WVC, AOD, TCC, and LCC. For Group 1, increases in E_g were observed at the Yining and Yanqi stations. For Group 2, decreases in E_g and increases in WVC, AOD, TCC, and LCC were observed at the Ruoqiang station. For Group 3, decreases in E_g and WVC and increases in AOD, TCC, and LCC were observed at the Urumqi, Tacheng, and Aksu stations. For Group 4, decreases in E_g and AOD and increases in WVC, TCC, and LCC were observed at the Altai, Kashgar, and Hetian stations. For Group 5, decreases in E_g and LCC and increases in WVC and TCC were observed at the Hami station. For Group 6, decreases in E_g, WVC, AOD, and TCC and increases in the LCC were observed at the Turpan station. To analyze the main drivers of E_g variations in Xinjiang, the Yining, Ruoqiang, Urumqi, Hetian, Hami, and Turpan stations were chosen from each group as a sample (Figure 5).

Figure 5 and Table 2 show that increasing trends in E_g at rates of 1.14×10^{-1} and 1.87×10^{-1} MJ·m^{-2}·decade^{-1} were observed at the Yining and Yanqi stations, respectively. The WVC decreased by -11.34×10^{-4} and -11.51×10^{-4} mm·decade^{-1} at these stations, respectively. Decreasing trends for the TCC at -1.04×10^{-3} mm and-0.22×10^{-3} mm·decade^{-1} were also observed at the Yining and Yanqi stations, respectively. Therefore, the decreases in the WVC and TCC might have caused the E_g brightening in Group 1.

A decreasing trend for E_g at a rate of -1.68×10^{-1} MJ·m^{-2}·decade^{-1} was observed at the Ruoqiang station in Group 2. Increasing trends for the WVC, AOD, TCC, and LCC at rates of 9.32×10^{-4} mm·decade^{-1}, 1.64×10^{-4}·decade^{-1}, 0.14×10^{-3}%·decade^{-1}, and 0.66×10^{-3}%·decade^{-1}, respectively, were also observed at the Ruoqiang station. Therefore, the increases in the WVC, AOD, TCC, and LCC might have caused the E_g glooming in Group 2 (Figure 5 and Table 2).

Decreasing trends for E_g at rates of -3.58×10^{-1}, -6.42×10^{-1}, and -4.31×10^{-1} MJ·m^{-2}·decade^{-1} were observed at the Urumqi, Tacheng, and Aksu stations, respectively, in Group 3. Decreasing trends were also observed for the WVC in Group 3, the highest rate of which was-33.70×1^{-4}% decade^{-1}. Increasing trends for the AOD, TCC, and LCC showed the highest rates of 33.97×10^{-4}·decade^{-1}, 17.04×10^{-3}%·decade^{-1}, and 15.42×10^{-3}% decade^{-1} at the Urumqi, Aksu, and Aksu stations, respectively. Therefore, the increases in the AOD, TCC, and LCC could have caused the E_g glooming in Group 3 (Figure 5 and Table 2).

Decreasing trends for E_g at rates of -2.13×10^{-1}, -2.30×10^{-1}, and -1.28×10^{-1} MJ·m^{-2}·decade^{-1} were observed at the Altai, Kashgar, and Hetian stations, respectively, in Group 4. A decreasing trend for the AOD was also observed in Group 4, with the highest rate of -1.10×10^{-4}·decade^{-1}. Increasing trends for the WVC, TCC, and LCC at the highest rates of 6.85×10^{-4} mm·decade^{-1}, 4.47×10^{-3}%·decade^{-1}, and 8.11×10^{-3}%·decade^{-1} were observed at the Altai, Kashgar, and Kashgar stations, respectively. Therefore, the increases in the TCC and LCC might have caused the E_g glooming in Group 4 (Figure 5 and Table 2).

A decreasing trend for E_g at a rate of -4.08×10^{-1} MJ·m^{-2}·decade^{-1} was observed at the Hami station in Group 5. A decreasing trend for the LCC was also found in Group 5 at a rate of -3.21×10^{-3}% decade^{-1}. Increasing trends for the WVC and TCC at rates of 6.85×10^{-4} mm·decade^{-1} and 2.88×10^{-3}%·decade^{-1}, respectively, were observed at the Hami station. Therefore, the increases in the WVC and TCC might have caused the E_g glooming in Group 5 (Figure 5 and Table 2).

A decreasing trend for E_g at a rate of -4.67×10^{-1} MJ·m^{-2}·decade^{-1} was observed at the Turpan station in Group 6. Decreasing trends for WVC, AOD, and LCC were also found in Group 6 at rates of -3.01×10^{-4} mm decade^{-1}, -4.11×10^{-4}·decade^{-1}, and -1.48×10^{-3}%·decade^{-1}, respectively. An increasing trend for the LCC was observed at a rate of 1.51×10^{-3}%·decade^{-1}. Therefore, the increases in the LCC might have caused the E_g glooming in Group 6 (Figure 5 and Table 2).

4. Discussion

Observations have indicated solar radiation dimming in most parts of the world in the 1950s–1990s, with decreasing values between −2.3 and −5.1 Wm^{-2}·decade^{-1} recorded at

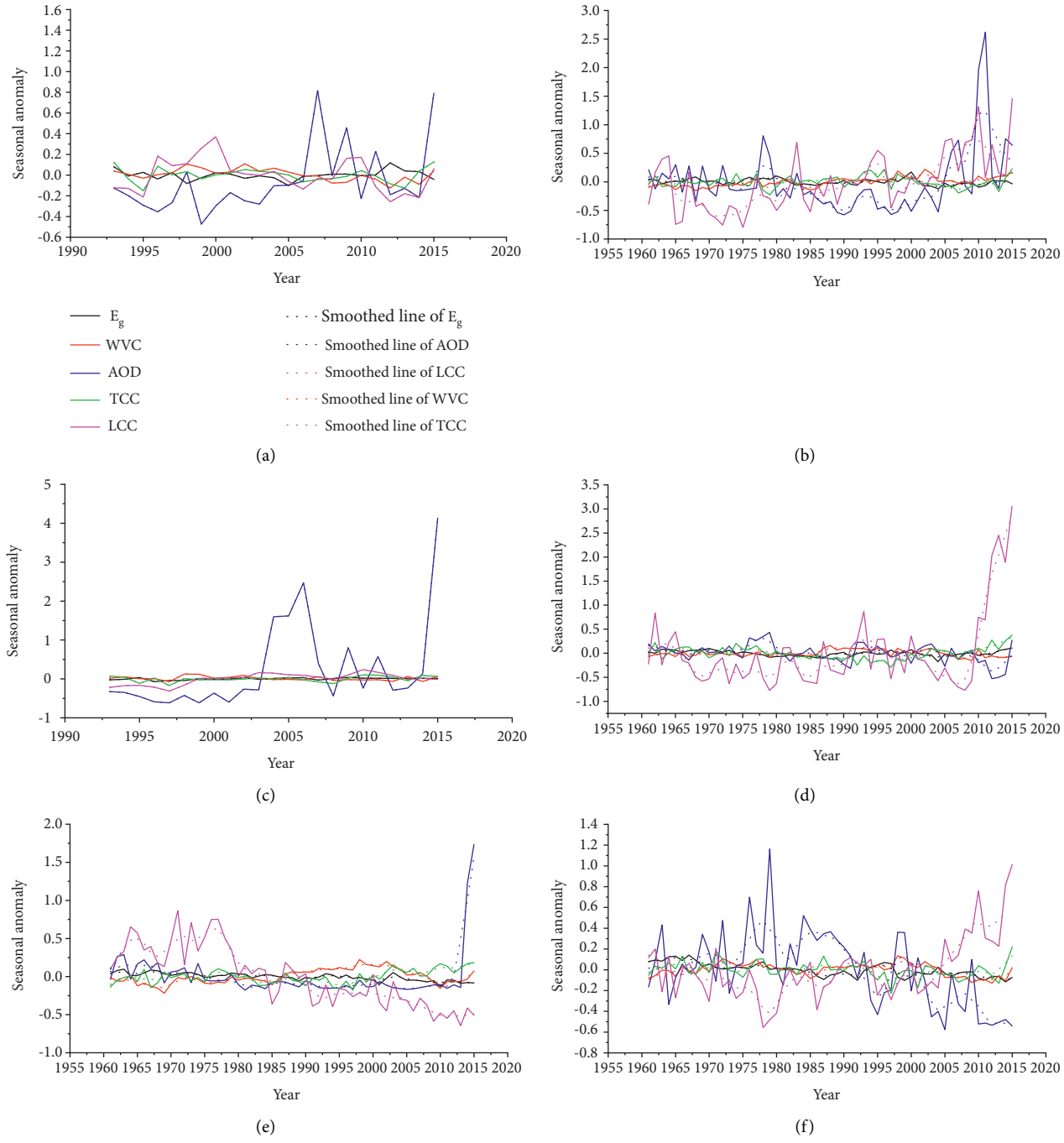

FIGURE 5: Interannual variations in anomalies of E_g (black solid lines), WVC (red solid lines), and AOD (blue solid lines) smoothed by the Lowess algorithm (dashed lines) observed at the (a) Yining, (b) Ruoqiang, (c) Urumqi, (d) Hetian, (e) Hami, and (f) Turpan stations in Xinjiang.

global sites [1, 2, 4]. However, the solar radiation in most parts of the world brightened during the 1980s–2000s with an increasing value of 2.2 Wm^{-2}·$decade^{-1}$at 352 sites. In the 1990s–2000s, the increasing values were 5.1 and 6.6 Wm^{-2}·$decade^{-1}$at 17 and 8 sites, respectively [43–45].

In Asia, the solar radiation trends were −1 to −8 and −2.9 Wm^{-2}·$decade^{-1}$ during 1960–1987 and 1966–1990 in the former Soviet Union and India at 160 and 10 sites, respectively [46, 47]. The decreasing trend values of solar radiation were −3.2 to−3.8, −7, and −4.5 to −4.9 Wm^{-2}·$decade^{-1}$ during the 1950s–2000s and 1960s–1980s in China at 85 and 84 sites, 84 sites, and 64 and 42 sites, respectively [6, 9, 11, 48]. The largest decreasing trend was −18 Wm^{-2}·$decade^{-1}$ at Hong Kong between 1958 and 1992 at one site [49]. However, increasing trends of solar radiation were 2.7 and 8.9 Wm^{-2}·$decade^{-1}$ in Asia during the

1990s–2000s at 84 and 86 sites, respectively [11, 17, 50, 51]. During the 1980s–2000s and 2000–2005, the decreasing trends were −8.6 and −4.2 Wm^{-2}·$decade^{-1}$ in India and China, respectively, at 12 sites [18, 52]. During the 1990s–2000s, the decreasing trends were 7.7–8.9 Wm^{-2}·$decade^{-1}$ in Japan [17, 50].

In Europe, the solar radiation trends were −2.7 and −3.1 Wm^{-2}·$decade^{-1}$ during the 1950s–1980s and 1970s–1980s at 13 and 75 sites, respectively [53, 54]. The largest decreasing trend was −8.8 Wm^{-2}·$decade^{-1}$ in Israel during 1954–1994 at two sites [55]. However, increasing trends of solar radiation at 1.4 and 3.3 Wm^{-2}·$decade^{-1}$ during the 1980s–2000s were noted in Europe at 75 and 133 sites, respectively [18, 53].

In the Americas, the solar radiation trends were −2.6 and −6 to−10 Wm^{-2}·$decade^{-1}$ during the 1950s–1990s and 1960s–1990s at 7 sites and 43 and 30 sites, respectively [2, 56, 57]. However, an increasing trend of 8 Wm^{-2}·$decade^{-1}$ occurred during 1995–2007 in the continental United States [58].

In Africa, the decreasing trends in solar radiation were −5.4 to −13 Wm^{-2}·$decade^{-1}$ during the 1960s–1990s at 10 sites and 1 site [59, 60].

In Australia, the trend value of solar radiation was −4.8 Wm^{-2}·$decade^{-1}$during the 1950s–1990s at four sites in New Zealand. However, an increasing trend of solar radiation at 0.5 Wm^{-2}·$decade^{-1}$ during the 1990–2008 also occurred in New Zealand [61].

In Antarctica and the Arctic regions, decreasing trend values in solar radiation at −2.8 and −3.6 Wm^{-2}·$decade^{-1}$ occurred during the 1950s–1990s at 12 and 22 sites, respectively [55, 62]. However, at the South Pole, the increasing trend of solar radiation was 4.1 Wm^{-2}·$decade^{-1}$ during the 1990s–2000s [17].

In Xinjiang, the glooming trend in solar radiation was the same as that in most parts of the world during 1961–2015, with a rate of -33.88×10^{-2} $MJ{\cdot}m^{-2}$·$decade^{-1}$ (-9.28×10^{-4} Wm^{-2}·$decade^{-1}$). The annual E_g strongly decreased during 1961–1992 at a rate of −0.60 $MJ{\cdot}m^{-2}$ $decade^{-1}$ (-1.64×10^{-3} Wm^{-2}·$decade^{-1}$). Afterward, the annual E_g weakly decreased during 1993–2015 at a rate of −0.22 $MJ{\cdot}m^{-2}$·$decade^{-1}$ (-0.60×10^{-3} Wm^{-2}·$decade^{-1}$). That is, after the 1990s, the variation in solar radiation in Xinjiang showed a decreasing trend that differed slightly from that in other parts of the world.

The WVC, AOD, TCC, and LCC are the main factors affecting the ability of solar radiation to reach the Earth's surface. The AOD, TCC, and LCC showed increasing trends, which could have caused the glooming of solar radiation in Xinjiang. It is interesting to note that 16.74%, 108.8%, 34.24%, and 216.34% increases in the WVC, AOD, TCC, and LCC decreased E_g by 9.43% between 1961 and 2015. The dimming trend of solar radiation was more obvious in autumn and winter, with the AOD and LCC in winter showing strong correlation with the solar radiation at the 95% level (Table 1). The causes of E_g changes differed among the groups. The decreasing WVC and TCC might have caused the E_g brightening at the Yining and Yanqi stations between 1993 and 2012. Further analysis revealed that 15.6% (8%) and 6.4% (22%) decreases in WVC and TCC increased E_g by 3.5% (2.7%) between 1961 and 2015 in Yining (Yanqi). However, the increases in the AOD, TCC, and LCC might have caused the E_g glooming at the Ruoqiang, Urumqi, Tacheng, and Aksu stations, whereas the increases in the TCC and LCC might have caused that at the Hami and Turpan stations.

5. Conclusions

Based on the observation data of 11 solar radiation stations in Xinjiang recorded during 1961–2015, this study analyzed the characteristics and influencing factors of solar radiation changes in this region. The results are summarized below.

(1) The E_g value showed characteristics of interdecadal variation, with values of 16.83, 16.37, 15.68, 15.54, 15.28, and 15.35 $MJ{\cdot}m^{-2}{\cdot}day^{-1}$ occurring in the 1960s, 1970s, 1980s, 1990s, 2000s, and 2010s. E_g showed a downward trend at a rate of -33.88×10^{-2} $MJ{\cdot}m^{-2}$·$decade^{-1}$ during 1961–2015, which represents a decrease of 9.43%. The trend rates in spring, summer, autumn, and winter were -1.92×10^{-2}, -1.89×10^{-2}, -3.47×10^{-2}, and -3.56×10^{-2} $MJ{\cdot}m^{-2}$·$decade^{-1}$, respectively.

(2) Increases in the WVC, AOD, LCC, and TCC occurred at rates of 7.12×10^{-5} mm·$decade^{-1}$, 2.74×10^{-6} $decade^{-1}$, 5.73×10^{-5}% $decade^{-1}$, and 8.77×10^{-5}% $decade^{-1}$, respectively, during 1961–2015. The annual variation in E_g was affected by the WVC, AOD, LCC, and TCC. The decrease in E_g in spring was affected by the WVC and LCC; that in summer was affected by the WVC, LCC, and TCC; and that in autumn and winter was affected by the WVC, AOD, LCC, and TCC.

(3) The spatial distribution of E_g in Xinjiang was complex. E_g at the Yining and Yanqi stations showed an increasing trend, whereas that at other stations showed a decreasing trend. The highest decreasing trend of -6.42×10^{-1} $MJ{\cdot}m^{-2}$·$decade^{-1}$ was recorded at the Tacheng station, whereas the lowest decreasing trend of -1.28×10^{-1} $MJ{\cdot}m^{-2}$·$decade^{-1}$ was recorded at the Hetian station. The 11 stations were divided into six groups, each of which had different impact factors for the E_g variations. An increase in E_g was observed in Group 1 in association with decreases in the WVC and TCC. A decrease in E_g was observed in Group 2, which might have been influenced by increases in the WVC, AOD, TCC, and LCC. The AOD, TCC, and LCC might have contributed to a decrease in E_g in Group 3. A decreasing trend in E_g was observed in Group 4 (Group 5), which might have been influenced by the WVC, TCC, and LCC (WVC and TCC). A decreasing trend in E_g influenced by the LCC was observed in Group 6.

Data Availability

The raw data are shared in the Institute of Desert Meteorology, China Meteorological Administration.

Additional Points

The code used in this study was developed by Zhenjie Li.

Ethical Approval

This study is based on freely accessible data that follow proper research ethics.

Consent

The authors confirm that the study is original and within the regulations for publication.

Conflicts of Interest

The authors declare no conflicts of interest regarding the publication of this paper.

Authors' Contributions

All authors contributed to the study's conception and design. Data collection of the manuscript was performed by Qing He. The drafts of the manuscript were written by Lili Jin. Lili Jin and Zhenjie Li provided all of the necessary explanations and suggestions for improving the manuscript. Alim Abbas drew Figures 1 and 4.

Acknowledgments

This work was supported by the Third Xinjiang Scientific Expedition and Research Program (Grant no. 2021xjkk030501) and the National Natural Science Foundation of China (nos. 42030612 and 41830968).

References

[1] H. Gilgen, M. Wild, and A. Ohmura, "Means and trends of shortwave irradiance at the surface estimated from global energy balance archive data," *Journal of Climate*, vol. 11, no. 8, pp. 2042–2061, 1998.

[2] B. G. Liepert, "Observed reductions of surface solar radiation at sites in the United States and worldwide from 1961 to 1990," *Geophysical Research Letters*, vol. 29, no. 10, 2002.

[3] J. Ma, H. Liang, Y. Luo, and S. K. Li, "Variation trend of direct and diffuse radiation in China over recent 50 years," *Acta Physica Sinica*, vol. 60, no. 6, pp. 069601–069614, 2011.

[4] G. Stanhill and S. Cohen, "Global dimming: a review of the evidence for a widespread and significant reduction in global radiation with discussion of its probable causes and possible agricultural consequences," *Agricultural and Forest Meteorology*, vol. 107, no. 4, pp. 255–278, 2001.

[5] M. Wild, H. Gilgen, A. Roesch et al., "From dimming to brightening: decadal changes in solar radiation at Earth's surface," *Science*, vol. 308, no. 5723, pp. 847–850, 2005.

[6] F. Liang and X. A. Xia, "Long-term trends in solar radiation and the associated climatic factors over China for 1961–2000," *Annales Geophysicae*, vol. 23, no. 7, pp. 2425–2432, 2005.

[7] S. P. Yang, K. L. Wang, and S. H. Lü, "Regional characteristics of global solar radiation evolution in China over recent 40 years," *Acta Energiae Solaris Sinica*, vol. 28, no. 3, pp. 227–232, 2007, (in Chinese).

[8] D. G. Streets, C. Yu, Y. Wu et al., "Aerosol trends over China, 1980–2000," *Atmospheric Research*, vol. 88, no. 2, pp. 174–182, 2008.

[9] H. Z. Che, G. Y. Shi, X. Y. Zhang et al., "Analysis of 40 years of solar radiation data from China, 1961-2000," *Geophysical Research Letters*, vol. 32, no. 6, Article ID L06803, 2005.

[10] Y. Qian, D. P. Kaiser, L. R. Leung, and M. Xu, "More frequent cloud-free sky and less surface solar radiation in China from 1955 to 2000," *Geophysical Research Letters*, vol. 33, no. 1, pp. 1–4, 2006.

[11] G.-Y. Shi, T. Hayasaka, A. Ohmura et al., "Data quality assessment and the long-term trend of ground solar radiation in China," *Journal of Applied Meteorology and Climatology*, vol. 47, no. 4, pp. 1006–1016, 2008.

[12] L. Zou, A. W. Lin, L. C. Wang et al., "Long-term variations of estimated global solar radiation and the influencing factors in Hunan province, China during 1980–2013," *Meteorology and Atmospheric Physics*, vol. 128, no. 2, pp. 155–165, 2016.

[13] S. L. Tao, Y. M. Qi, S. H. Shen, Y. H. Li, and Y. Zhou, "The spatial and temporal variation of solar radiation over China from 1981 to 2014," *Journal of Arid Land Resources & Environment*, vol. 30, no. 11, pp. 143–147, 2016.

[14] Z. H. Chen, G. Y. Shi, and H. Z. Chen, "Analysis of the solar radiation of Xinjiang uygur autonomous region in recent 40 years," *Arid Land Geography*, vol. 28, no. 6, pp. 734–739, 2005, (in Chinese).

[15] R. Li, L. Zhao, Y. J. Ding, and Y. Xiao, "A study of the effect of global radiation and other factors on seasonal maximum frozen depth in the Tibetan Plateau," in *Proceedings of the Power Engineering and Automation Conference*, Wuhan, China, September 2011.

[16] Q. He, Q. L. Miao, S. Li, L. Shi, and M. Ali, "Global radiation characteristics and influencing factors of Taklimakan desert hinterland," *Journal of Desert Research*, vol. 28, no. 5, pp. 896–902, 2008, (in Chinese).

[17] M. Wild, "Global dimming and brightening: a review," *Journal of Geophysical Research*, vol. 114, no. D10, pp. D00D16–31, 2009.

[18] M. Wild, "How well do IPCC-AR4/CMIP3 climate models simulate global dimming/brightening and twentieth- centurydaytime and nighttime warming?" *Journal of Geophysical Research*, vol. 114, Article ID D00D11, 2009.

[19] J. Almorox and C. Hontoria, "Global solar radiation estimation using sunshine duration in Spain," *Energy Conversion and Management*, vol. 45, no. 9-10, pp. 1529–1535, 2004.

[20] M. El-Metwally, "Sunshine and global solar radiation estimation at different sites in Egypt," *Journal of Atmospheric and Solar-Terrestrial Physics*, vol. 67, no. 14, pp. 1331–1342, 2005.

[21] M. G. Iziomon and H. Mayer, "Assessment of some global solar radiation parameterizations," *Journal of Atmospheric and Solar-Terrestrial Physics*, vol. 64, no. 15, pp. 1631–1643, 2002.

[22] M. Yorukoglu and A. N. Celik, "A critical review on the estimation of daily global solar radiation from sunshine duration," *Energy Conversion and Management*, vol. 47, no. 15-16, pp. 2441–2450, 2006.

[23] L. D. Wang, *Study of Shortwave Radiation Based on Situ Observation and Satellite Products over Tibetan Plateau[D]*, Lanzhou University, Lanzhou China, (in Chinese), 2012.

[24] Y. T. Liang, K. Q. Liu, and Z. H. Xia, "Estimation of solar radiation using FY-2C data," *Meteorological Science and Technology*, vol. 37, no. 2, pp. 234–238, 2009.

[25] W. Liu, H. P. Liu, and Y. P. Wang, "Estimation of dekad solar radiation with GMS-5 data," *Meteorology*, vol. 28, no. 6, pp. 35–38, 2002.

[26] C. Rigollier, M. Lefèvre, and L. Wald, "The method Heliosat-2 for deriving shortwave solar radiation from satellite images," *Solar Energy*, vol. 77, no. 2, pp. 159–169, 2004.

[27] K. Wang, H. Ye, F. Chen, Y. Z. Xiong, X. Y. Li, and L. N. Tang, "Long-term change of solar radiation in southeastern China: Variation, factors, and climate forcing," *Ecology and Environmental Sciences*, vol. 19, no. 5, pp. 1119–1124, 2010, (in Chinese).

[28] S. Yang, G. Y. Shi, B. Wang, H. L. Yang, and Y. X. Duan, "Trends in surface solar radiation (SSR) and the effect of clouds on SSR during 1961-2009 in China," *Chinese Journal of Atmospheric Sciences*, vol. 37, no. 5, pp. 963–970, 2013, (in Chinese).

[29] C. X. Zhao, Y. F. Zheng, R. J. Wu, and J. J. Liu, "Analysis of solar radiation and relative factors in Southeast coastal cities of China," *Journal of Tropical Meteorology*, vol. 29, no. 3, pp. 465–473, 2013, (in Chinese).

[30] J. Y. Ma, Y. Luo, H. Ling, and S. K. Li, "Spatial and temporal variation of total solar radiation in China in recent 50 years," *Journal of Natural Resources*, vol. 27, no. 2, pp. 268–280, 2012.

[31] J. Y. Ma, Y. Luo, Y. B. Shen, H. Liang, and S. K. Li, "Regional long-term trend of ground solar radiation in China over the past 50 years," *Science China Earth Sciences*, vol. 42, no. 10, pp. 1597–1608, 2012, (in Chinese).

[32] G. Stanhill and S. Moreshet, "Global radiation climate changes: the world network," *Climatic Change*, vol. 21, no. 1, pp. 57–75, 1992.

[33] D. Y. Zhou, H. H. Yang, R. Qin et al., "Study on surface solar radiation over Xinjiang Uygur Autonomous Region based on surface observation and the GEWEX-SRB retrieved from satellite," *Journal of Meteorology and Environment*, vol. 34, no. 4, pp. 84–91, 2018, (in Chinese).

[34] S. Q. Zhang and Z. C. Pu, "Study on temporal and spatial variation characteristics of reference evapotranspiration in Xinjiang," *Transactions of the CSAE*, vol. 27, no. 5, pp. 73–79, 2011.

[35] W. P. Liu, W. S. Wei, and X. L. Tang, "Variation of sunshine hour in recent 45 years in Aksu Prefecture," *Arid Land Geography*, vol. 31, no. 2, pp. 197–202, 2008.

[36] X. Yang, M. Cai, Y. Z. Zhao, Y. H. Zhang, A. Luo, and Y. A. Jiang, "Analysis on the change of sunshine duration in Kashgar, Xinjiang in recent 39 years," *Arid Zone Research*, vol. 28, no. 1, pp. 158–162, 2011.

[37] Y. Xin, Y. Z. Zhao, W. Y. Mao, Y. P. Li, X. M. Wang, and Y. P. He, "Homogeneity test of the total solar radiation data series and further research on climatological calculation over Xinjiang," *Plateau Meteorology*, vol. 30, no. 4, pp. 878–889, 2011.

[38] A. L. Xu, J. Li, H. Z. Liu, and J. H. Sun, "Quality control of surface radiation data measured in Dali National Climate Observatory," *Plateau Meteorology*, vol. 32, no. 5, pp. 1432–1441, 2013.

[39] Y. Fei, X. G. Xia, and H. Z. Che, "Dust aerosol drives upward trend of surface solar radiation during 1980–2009 in the Taklimakan Desert," *Atmospheric Science Letters*, vol. 15, no. 4, pp. 282–287, 2014.

[40] S. Qin, G. Shi, L. Chen et al., "Long-term variation of aerosol optical depth in china based on meteorological horizontal visibility observations," *Chinese Journal of Atmospheric Sciences*, vol. 34, no. 2, p. 7, 2010.

[41] P. F. Abbott and R. C. Tabony, "The estimation of humidity parameters," *The Meteorological Magazine*, vol. 114, no. 1351, pp. 49–56, 1985.

[42] X. Xia, "A closer looking at dimming and brightening in China during 1961–2005," *Annales Geophysicae*, vol. 28, no. 5, pp. 1121–1132, 2010.

[43] M. Wild, "Decadal changes in surface radiative fluxes and their importance in the context of global climate change," in *Climate Variability and Extremes During the Past 100 Years*, vol. 33, pp. 155–167, Springer, Berlin, Germany, 2008.

[44] M. Wild, H. Gilgen, A. Roesch et al., "From dimming to brightening: decadal changes in solar radiation at earth's surface," *Science*, vol. 308, no. 5723, pp. 847–850, 2005.

[45] M. Wild, "Global dimming and brightening: a review," *Journal of Geophysical Research: Atmospheres*, vol. 114, no. D10, pp. 1–13, 2009.

[46] G. M. Abakumova, E. M. Feigelson, V. Russak, and V. V. Stadnik, "Evaluation of long-term changes in radiation, cloudiness and surface temperature on the territory of the former Soviet Union," *Journal of Climate*, vol. 9, pp. 1319–1327, 1996.

[47] V. Ramanathan, C. Chung, D. Kim et al., "Atmospheric brown clouds: impacts on South Asian climate and hydrological cycle," *Proceedings of the National Academy of Sciences of the United States of America*, vol. 102, no. 15, pp. 5326–5333, 2005.

[48] Y. Qian, W. Wang, L. R. Leung, and D. P. Kaiser, "Variability of solar radiation under cloud-free skies in China: the role of aerosols," *Geophysical Research Letters*, vol. 34, no. 12, Article ID L12804, 2007.

[49] G. Stanhill and J. D. Kalma, "Solar dimming and urban heating at Hong Kong," *International Journal of Climatology*, vol. 15, no. 8, pp. 933–941, 1995.

[50] J. R. Norris and M. Wild, "Trends in aerosol radiative effects over China and Japan inferred from observed cloud cover, solar "dimming, " and solar "brightening," *Journal of Geophysical Research*, vol. 114, Article ID D00D15, 2009.

[51] A. Ohmura, "Observed long-term variations of solar irradiance at the earth's surface," *Space Science Reviews*, vol. 125, no. 1-4, pp. 111–128, 2006.

[52] B. Padma Kumari, A. L. Londhe, S. Daniel, and D. B. Jadhav, "Observational evidence of solar dimming: offsetting surface warming over India," *Geophysical Research Letters*, vol. 34, no. 21, Article ID L21810, 2007.

[53] J. R. Norris and M. Wild, "Trends in aerosol radiative effects over Europe inferred from observed cloud cover, solar "dimming, " and solar "brightening," *Journal of Geophysical Research*, vol. 112, no. D8, Article ID D08214, 2007.

[54] A. Ohmura and H. Lang, "Secular variation of global radiation over Europe," in *Current Problems in Atmospheric Radiation*, pp. 98–301, Deepak, Hampton, VA, USA, 1989.

[55] G. Stanhill and S. Cohen, "Recent changes in solar irradiance in Antarctica," *Journal of Climate*, vol. 10, no. 8, pp. 2078–2086, 1997.

[56] J. C. Antuña, A. Fonte, A. Rodríguez, and M. Wild, "Observed solar dimming in the wider caribbean," *Atmósfera*, vol. 24, no. 2, pp. 193–201, 2011.

[57] H. W. Cutforth and D. Judiesch, "Long-term changes to incoming solar energy on the Canadian prairie," *Agricultural and Forest Meteorology*, vol. 145, no. 3-4, pp. 167–175, 2007.

[58] C. N. Long, E. G. Dutton, J. A. Augustine et al., "Significant decadal brightening of downwelling shortwave in the continental United States," *Journal of Geophysical Research*, vol. 114, Article ID D00D06, 2009.
[59] M. A. Omran, "Analysis of solar radiation over Egypt," *Theoretical and Applied Climatology*, vol. 67, no. 3-4, pp. 225–240, 2000.
[60] H. C. Power and D. M. Mills, "Solar radiation climate change over southern Africa and an assessment of the radiative impact of volcanic eruptions," *International Journal of Climatology*, vol. 25, no. 3, pp. 295–318, 2005.
[61] J. B. Liley, "New Zealand dimming and brightening," *Journal of Geophysical Research*, vol. 114, Article ID D00D10, 2009.
[62] G. Stanhill, "Global irradiance, air pollution and temperature changes in the Arctic," *Philosophical Transactions of the Royal Society A*, vol. 352, pp. 247–258, 1995.